# Effect of Pressure on the Isotope Effect in Sodium Self-Diffusion*

John N. Mundy

*Argonne National Laboratory, Argonne, Illinois* 60439

The diffusion of $^{22}$Na in sodium has been measured over the temperature range $-78.5$ to 97°C and the data do not fit a linear Arrhenius relation. The data indicate that at least two, and possibly three, jump mechanisms could be responsible for the diffusion behavior. The diffusion of $^{22}$Na in sodium has been measured as a function of pressure over the range from ambient pressure to 9500 kg cm$^{-2}$ at 14.8 and 91.3 °C. The $\ln D$-vs-pressure results also show curvature and are in substantial agreement with the ambient-pressure data. Isotope-effect measurements have been made over the temperature-range $-25.0$ to 97 °C at ambient pressure. The isotope effect decreases as the temperature increases over the entire temperature range, with a more rapid decrease above 70 °C. Isotope-effect measurements have been made at 7000 kg cm$^{-2}$ over a temperature range 14.8–117 °C. The effect of pressure on the isotope effect is not large. The variation of isotope effect with temperature appears to be less at 7000 kg cm$^{-2}$. Collectively, the data are interpreted in terms of one, two, or three mechanisms of diffusion. It is not possible to determine unambiguously the mechanisms of diffusion in sodium. The evidence appears to favor a vacancy mechanism at low temperatures with an increasing contribution from divacancies as the melting temperature is approached.

## I. INTRODUCTION

The isotope effect in diffusion is observed by measuring the variation of tracer diffusion relative to the mass of the diffusing atom. Measurement of the isotope effect provides an important means of determining the diffusion mechanism. The equation for the isotope effect[1-] can be written in the following general form:

$$(D_{\alpha}/D_{\beta}) - 1 = f \Delta K \left[ (m_{\beta}/m_{\alpha})^{1/2} - 1 \right] , \qquad (1)$$

where $D_{\alpha}$, $m_{\alpha}$, and $D_{\beta}$, $m_{\beta}$ refer to the diffusion coefficient and mass of the $\alpha$ and $\beta$ isotope, respectively; $f$ is the correlation factor; $\Delta K$ is the fraction of the total translational kinetic energy associated with the decomposition of the saddle-point configuration that is possessed by the migrating atom.

For self-diffusion in cubic metals, $f$ is a geometric factor dependent only on the crystal structure and the atomic jump process. Measurements of $D_{\alpha}/D_{\beta}$ yield the product $f \Delta K$; thus, if $\Delta K$ is close to unity, the experimental results yield an unambiguous value of $f$, which serves to identify the diffusion mechanism. Measurements of the isotope effect in metals with a close-packed structure[4-12] have shown that diffusion occurs by means of vacancies. The most recent measurements,[5] however, showed that in silver, in the temperature region close to the melting point, a measurable fraction of the diffusion occurs by means of divacancies.[13]

Measurements of the isotope effect in bcc metals (sodium[14] and δ-Fe[10]) yielded such low values of $f \Delta K$ that it was not possible to identify, unambiguously, the mechanism of diffusion. In a search for further evidence to aid in an identification of the mechanism, it was noted "that there appeared to be a connection between values of $\Delta K$ and relative activation volumes" (activation volume relative to molar volume $\Delta V/V$).[14] Further experimental evidence appears to support this correlation. (All the experimental evidence is listed in Table I.) LeClaire[21] has established a connection between $\Delta K$ and $\Delta V/V$ on the basis of the relaxation that takes place around vacant lattice sites. Recent measurements of the activation volume for self-diffusion in zinc[17,18] do not support the correlation, and the present work investigates more closely the connection between $\Delta V/V$ and $\Delta K$.

The differences in diffusion behavior between close-packed metals and metals with a bcc structure are not confined to the strength of the isotope effect. A review of many of these differences can be found in Ref. 22. The evidence suggests that bcc metals can be divided into two groups. The first or "normal" group has the following characteristics: (i) a diffusion coefficient that follows the Arrhenius equation as a function of temperature; (ii) a $D_0$ between 0.1 and 10; and (iii) a value of the activation energy $Q$ that approximately follows the melting-point rule. The "normal" bcc metals are Li, Na, K, Fe, Nb, Mo, Ta, and W. The second or "anomalous" group does not have the above characteristics and consists of $\beta$-Ti, $\beta$-Zr, $\beta$-Hf, $\gamma$-U, V, $\beta$-Pr, $\epsilon$-Pu, and Cr.

This work was undertaken to obtain a greater understanding of the diffusion processes in bcc metals. Sodium was chosen for many reasons. The experimental techniques were well established, and extensive data on sodium were available. Since sodium is such a highly compressible material, it was hoped that changes brought about in the pressure

TABLE I. Isotope effect for self-diffusion in pure metals.

| Element | Structure | Isotopes | $\Delta K$ | $\Delta V/V$ | Ref. |
|---------|-----------|----------|------------|--------------|------|
| Cu | fcc | $Cu^{67}$, $Cu^{64}$ | $0.87 \pm 0.02$ | 0.90 | 6, 15 |
| Ag | fcc | $Ag^{105}$, $Ag^{110}$ | $0.86 \pm 0.02$ | 0.90 | 5, 16 |
| Pd | fcc | $Pd^{103}$, $Pd^{112}$ | $1.02 \pm 0.04$ | $\cdots$ | 7 |
| Zn | hcp | $Zn^{65}$, $Zn^{69}$ | $0.93 \pm 0.03$ | 0.43 | 8, 17 |
|    |     | $Zn^{65}$, $Zn^{69}$ | $0.88 \pm 0.03$ | 0.43 | 9, 18 |
| $\gamma$-Fe | fcc | $Fe^{52}$, $Fe^{59}$ | $0.68 \pm 0.02$ | $\cdots$ | 10 |
|    |     | $Fe^{55}$, $Fe^{59}$ | $0.74 \pm 0.08$ | 0.77 | 11, 19 |
| $\delta$-Fe | bcc | $Fe^{52}$, $Fe^{59}$ | $0.46 \pm 0.01$ | $\cdots$ | 10 |
| Na | bcc | $Na^{22}$, $Na^{24}$ | $0.50 \pm 0.05$ | 0.52 | 14, 20 |

range 0–10 000 kg cm$^{-2}$ could be readily measurable. Measurements of the activation volume for self-diffusion in sodium, made by Nachtrieb et al.,[20] indicated that $\Delta V/V$ varied with applied pressure. Measurements of the variation of the isotope effect with pressure could shed light on the correlation between $\Delta K$ and $\Delta V/V$.

## II. EXPERIMENTAL METHODS

The experimental methods used were essentially the same as those described by Mundy et al.[14] Modifications were necessary to make the high-pressure diffusion anneals and to improve the overall accuracy of the isotope-effect measurements. The latter was required so that the small variations caused by temperature and pressure could be observed. Only the differences from the previous experimental method will be described.

### A. Materials

The sodium, with a purity of 5N5, was distilled at Argonne. The metal was kept under argon in a stainless-steel reservoir from which measured amounts could be passed through a stainless-steel frit and cast into the hand microtome. The melting point of the sodium was 97.9 ± 0.1 °C. Active sodium was prepared from $^{22}NaCl$ and $^{24}Na_2CO_3$ purchased from Nuclear Science Division, International Chemical and Nuclear Corporation. Analysis of the isotopes with a multichannel analyzer and a Ge(Li) detector showed no detectable radioactive impurities. The half-life of 2.6 yr for $^{22}Na$, as stated in the literature,[23] was adopted. The half-life of 14.98 h for $^{24}Na$ was the mean of many measurements in our own counting systems.

### B. Diffusion Measurements

The deposition of the radioactive tracers on a clean sodium surface and the ambient pressure anneals were performed as previously described.[14] After evaporation, the sample to be annealed under pressure was transferred under dry helium to the high-pressure cell. The cell was supplied by Harwood Engineering Co., Waltham, Mass. This company also supplied the manganin-resistance pres-

sure gauges used to measure the gas pressure. One gauge, attached to a recorder, continuously recorded the pressure. The other gauge, located close to the high-pressure diffusion cell, was connected to a Carey-Foster bridge. By use of the bridge and the calibration chart supplied by Harwood, the pressure could be measured to ± 25 psi. The high-pressure diffusion cell contained three iron-constantan thermocouples so that the temperature of the diffusion sample could be closely monitored. The pressure was generated with nitrogen or helium gas using pressure-generating equipment supplied by Autoclave Engineering Co., Erie, Pa. We found that, in the majority of the experiments, pressure could be maintained in a closed system, i.e., the leakage rate was too small to measure.

The sequence of operations for a high-pressure anneal were as follows. The evaporation of the active layer was made onto a precooled (− 25 °C) sample, and the temperature of the sample was monitored with a copper-constantan thermocouple. The sample was transferred to the high-pressure cell that was also cooled (15 °C), and the temperature was monitored by one of the iron-constantan thermocouples. The pressure was raised to the desired point, with appropriate allowance made for the increase in pressure on heating the cell. After a pause of a few minutes to ascertain that the system was "leak-tight," the temperature was raised. The cell was designed with a heat-transfer jacket to enable 75 lb of steel to be rapidly heated and thus reduce errors in the measurement of "time at temperature." Boiling water or superheated steam could be passed through this jacket so that the anneal temperature could be attained in approximately 20 min. When the sample reached the anneal temperature, the hot water could be turned off and an oil bath raised to completely surround the high-pressure cell. The oil bath was set at the desired temperature and controlled to ± 0.05 °C. With reasonable care, the sample was within ± 0.1 °C of the controlled temperature in 30 min. The temperature of the anneal was determined by mercury in glass thermometers placed in the oil bath. These thermometers and all thermocouples used in this

work had been calibrated against a standardized platinum thermometer. At all times, agreement between thermocouples and thermometers were within 0.1 °C. A correction was made for the effect of pressure on the iron-constantan thermocouples using the data of Hannemann and Strong.[24] At the highest temperatures and pressures, the pressure decreased the thermocouple emf an amount equivalent to 0.2 °C. Although scatter on the order of ± 0.05 °C was present in our values, they were in agreement with the data of Hannemann and Strong. At the end of the anneal, the oil bath was lowered and the sample cooled to room temperature in approximately 20 min by forcing cold water through the heat-transfer jacket. The pressure was released and the sample removed, transferred to the dry box, quenched in a few minutes to − 45 °C, and sectioned at this temperature. Using this annealing procedure, the "heat up" and quench times were kept to a small fraction of the total time of anneal. Using the data of Nachtrieb et al.[20] corrections were made for these heating and cooling times allowing for the variations due to pressure. It should be emphasized that appreciable diffusion in sodium occurs at room temperature. The temperature and pressure of the sample must be monitored from the time of evaporation to the completion of sectioning, and also a carefully planned anneal procedure must be followed. In this way, we could determine all the anneal times to within 0.5%, provided the experiments ran at least for $1.5 \times 10^4$ sec.

The shape of the sample holder was designed so that, with a careful casting procedure, the samples did not undergo visible deformation due to the pressure anneal. Small deformation could be expected to be critical since the pressures used decrease the sample length an appreciable fraction of the diffusion zone. A "cusping" of 100 $\mu$ over the surface of the $\frac{3}{4}$-in.-diam sample was sufficient to nullify the results. As an example of this effect, a value of the isotope effect at 40 °C and 7000 kg cm$^{-2}$ pressure is given in the experimental results. This concavity or cusping had been observed in the earlier ambient-pressure work but the problem amplified with application of pressure. This deformation was found to be due to the presence of small voids that were extremely difficult to detect. Because of these deformations, each sample was given a pressure-temperature anneal before the diffusion anneal and only undeformed samples were used.

After the diffusion anneals, the samples were sectioned with a hand microtome. The 10-$\mu$ sections had to be cut with a precision similar to the 100-$\mu$ sections previously described[14] because of the decrease in the diffusion coefficient with pressure and the greater accuracy required. This was achieved by cutting at a lower temperature (− 45 °C) using a microtome with considerably finer adjust-

ment and with heavier cutting blades. This improvement allowed the diffusion measurements to be extended to − 78.5 °C, the isotope-effect experiments to − 25.0 °C, and made possible the pressure measurements over a wide range of pressure and temperature.

The sections were allowed to oxidize and then were dissolved in 1 ml of dilute HCl. The radiation from each section was counted to $10^5$ counts over background in a well-type scintillation counter. After counting, the sections were taken to dryness and the weight of the salt (NaCl) was measured. The section thickness and the specific activities were determined from the weights. This procedure overcame the problem of weighing the rapidly oxidizing sodium metal slice.

### C. Isotope-Effect Measurements

The same techniques were used for the diffusion anneals and sectioning as in the diffusion measurements; however, a different counting procedure was used. The ratio of the concentration of $^{22}$Na to $^{24}$Na was determined in each section by a half-life separation described in detail by Rothman and Peterson.[25] Each section was counted to $10^6$ counts, six or more times in the 5 days immediately following the sectioning. Corrections accurate to 0.1% were made for background, counter dead time, and counter drift. To ensure that the counting equipment behaved linearly, "null experiments" were performed. For this experiment, aliquots of $^{24}$NaCl/$^{22}$NaCl taken from the standard mixture and covering the entire activity range were counted in the same manner as the sections from a diffusion sample. These experiments showed that the variation of isotopic ratio with counting rate was less than the standard error of the slope for a diffusion sample.

### III. EXPERIMENTAL RESULTS

The solution of the diffusion equation for the experimental conditions used in this work is

$$c_x = c_0 e^{-x^2/4Dt} , \qquad (2)$$

where $c_x$ is the specific activity of the tracer at a distance $x$ from the surface, $t$ is the time of anneal, and $D$ is the diffusion coefficient. The two examples of penetration profiles of $^{22}$Na in sodium shown in Fig. 1 are typical of those obtained in this work. These particular profiles are shown as a comparison of data obtained at approximately the same temperature (80 °C) but at greatly different pressures (ambient and 7000 kg cm$^{-2}$).

### A. Diffusion as a Function of Temperature at Ambient Pressure

Values of the diffusion coefficient were obtained by computer from a least-squares fit of the data to
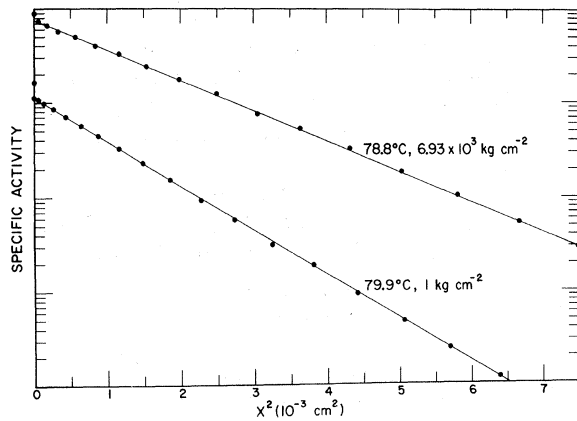
FIG. 1.  Concentration profiles for diffusion of $^{22}$Na into sodium.

TABLE III.  Diffusion of $^{22}$Na in sodium as a function of pressure.

| $T = 14.8\,°C$ | | $T = 91.3\,°C$ | |
|---|---|---|---|
| $D$ (cm$^2$ sec$^{-1}$) | Pressure (kg cm$^{-2}$) | $D$ (cm$^2$ sec$^{-1}$) | Pressure (kg cm$^{-2}$) |
| $3.23 \pm 0.03 \times 10^{-9}$ | 1 | $1.34 \pm 0.01 \times 10^{-7}$ | 1 |
| $1.57 \pm 0.01 \times 10^{-9}$ | 1638 | $8.04 \pm 0.03 \times 10^{-8}$ | 1291 |
| $9.21 \pm 0.09 \times 10^{-10}$ | 2951 | $5.26 \pm 0.02 \times 10^{-8}$ | 2464 |
| $4.41 \pm 0.02 \times 10^{-10}$ | 5089 | $5.24 \pm 0.03 \times 10^{-8}$ | 2500 |
| $2.39 \pm 0.02 \times 10^{-10}$ | 6889 | $3.31 \pm 0.05 \times 10^{-8}$ | 3833 |
| $2.29 \pm 0.20 \times 10^{-10}$ | 6943 | $2.04 \pm 0.01 \times 10^{-8}$ | 5758 |
| $1.57 \pm 0.01 \times 10^{-10}$ | 8064 | $1.81 \pm 0.01 \times 10^{-8}$ | 5770 |
| $1.01 \pm 0.01 \times 10^{-10}$ | 9464 | $1.15 \pm 0.01 \times 10^{-8}$ | 7709 |
| | | $8.62 \pm 0.02 \times 10^{-9}$ | 8901 |

Eq. (2).  Errors in $D$ arise from both scatter in the penetration profile and measurement of time.  Since these errors vary from run to run, individual errors are quoted with the values of $D$ in Tables II

TABLE II.  Diffusion of $^{22}$Na and $^{24}$Na in sodium as a function of temperature.

| Temperature (°C) | $D$ (cm$^2$ sec$^{-1}$) | $[(D_{22}/D_{24}) - 1]$ |
|---|---|---|
| 97.2 | $1.86 \pm 0.02 \times 10^{-7}$ | $0.0133 \pm 0.0003$ [a] |
| 95.9 | $1.71 \pm 0.30 \times 10^{-7}$ [b] | $0.0115 \pm 0.0002$ |
| 95.7 | $1.64 \pm 0.05 \times 10^{-7}$ | $0.0100 \pm 0.0060$ [a] |
| 94.5 | $1.51 \pm 0.03 \times 10^{-7}$ | a |
| 92.6 | $1.34 \pm 0.20 \times 10^{-7}$ [b] | $0.0110 \pm 0.0020$ [a] |
| 89.7 | $1.27 \pm 0.01 \times 10^{-7}$ | |
| 89.6 | $1.21 \pm 0.03 \times 10^{-7}$ | $0.0137 \pm 0.0005$ [a] |
| 87.6 | $1.12 \pm 0.02 \times 10^{-7}$ | a |
| 84.2 | $9.94 \pm 0.01 \times 10^{-8}$ | $0.0140 \pm 0.0004$ |
| 84.0 | $9.81 \pm 0.07 \times 10^{-8}$ | $0.0161 \pm 0.0016$ [a] |
| 79.9 | $8.31 \pm 0.08 \times 10^{-8}$ | $0.0151 \pm 0.0002$ |
| 72.0 | $5.79 \pm 0.03 \times 10^{-8}$ | $0.0158 \pm 0.0004$ [a] |
| 63.2 | $3.33 \pm 0.40 \times 10^{-8}$ [b] | $0.0163 \pm 0.0018$ [a] |
| 54.9 | $2.65 \pm 0.02 \times 10^{-8}$ | $0.0172 \pm 0.0013$ [a] |
| 40.0 | $1.34 \pm 0.02 \times 10^{-8}$ | $0.0162 \pm 0.0006$ [a] |
| 40.0 | $1.32 \pm 0.01 \times 10^{-8}$ | $0.0166 \pm 0.0002$ |
| 35.0 | $1.02 \pm 0.02 \times 10^{-8}$ | a |
| 34.7 | $9.66 \pm 0.01 \times 10^{-9}$ | $0.0167 \pm 0.0002$ |
| 25.2 | $5.81 \pm 0.10 \times 10^{-9}$ | a |
| 12.1 | $2.63 \pm 0.02 \times 10^{-9}$ | |
| 0.1 | $1.35 \pm 0.01 \times 10^{-9}$ | $0.0173 \pm 0.0003$ |
| 0.0 | $1.34 \pm 0.01 \times 10^{-9}$ | a |
| 0.0 | $1.32 \pm 0.01 \times 10^{-9}$ | a |
| −14.3 | $5.20 \pm 0.02 \times 10^{-10}$ | |
| −25.5 | $2.08 \pm 0.02 \times 10^{-10}$ | $0.0171 \pm 0.0004$ |
| −37.5 | $8.69 \pm 0.10 \times 10^{-11}$ | |
| −50.3 | $2.65 \pm 0.06 \times 10^{-11}$ | |
| −65.0 | $6.97 \pm 0.05 \times 10^{-12}$ | |
| −78.6 | $1.59 \pm 0.04 \times 10^{-12}$ | |

[a] Values from Ref. 14.
[b] Values not used in least-squares fit.

and III.  The errors in $D$ do not include the error in the measurement of the sample area.  The cross-sectional area of the sample space in the hand microtome is used in the calculation of the section thickness.  Although as much care as possible is taken to ensure that the sodium sample fills the microtome, the problems that arise could result in an error in $D$ on the order of 1%.  Table II contains both the present data and the previous data of Ref. 14.  These data are plotted in Fig. 2 and, as can be noted, the data do not follow a simple Arrhenius relation,

$$D = D_0 e^{-Q/kT} . \tag{3}$$

At least two diffusion processes appeared to be operating over the measured temperature range of $-78.6\,°C$ to the melting point.  An analysis was made by computer, using a variable metric fitting routine,[26] to fit the data to first a two- and then a three-exponential equation.  Three values in Table II were not used in these calculations because of large errors.  The two-exponential fit of the temperature data yields the following equation:

$$D = 0.72 \pm 0.05 \exp\left(-\frac{11500 \pm 500}{kT}\right)$$

$$+ 0.0057 \pm 0.0004 \exp\left(-\frac{8530 \pm 200}{kT}\right). \tag{4}$$

The three-exponential fit to the temperature data is far less satisfactory.  The six parameters could be changed over a wide range with little change in the goodness of fit.  The following equation was chosen because it had a good fit and, at the same time, yielded percentages of the low process that were in agreement with the temperature and pressure data:

$$D = 8.0\, e^{-14\,000/kT} + 0.144\, e^{-10\,840/kT}$$
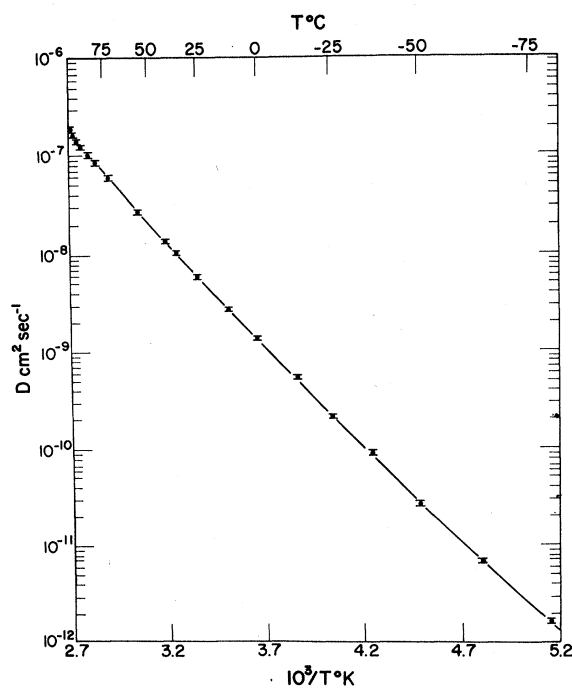
$$+ 0.009\, e^{-8720/kT} . \tag{5}$$

FIG. 2. Diffusion of $^{22}$Na in sodium as a function of
temperature.

The calculated errors in these six parameters are
not quoted. The errors are similar in magnitude
to those quoted for the two-exponential fit but are
unrealistic because the parameters can change over
a much wider range with an insignificant change in
the goodness of fit.

### B. Diffusion as a Function of Pressure at 14.8 and 91.3°C

The two- and three-exponential fits to the tem-
perature data indicated that, at low temperatures,
diffusion was predominantly by one mechanism but
close to the melting point this mechanism only con-
tributed approximately one-third of the diffusion.
It was decided to measure the variation of diffusion
coefficient with pressure at two temperatures,
which differed as much as was reasonably prac-
ticable. The temperatures used were 91.3 and
14.8 °C and the data obtained are given in Table III
and plotted in Fig. 3.

The variation of diffusion with pressure was not
linear, therefore, the data were fitted to both a
two- and three-exponential equation, using the same
procedure as with the temperature data. These fits
yield values of the activation volume for each pro-
cess and also the percentage of each process con-
tributing to diffusion at ambient pressure.

The activation volume is defined, in general, as
the pressure coefficient of the Gibbs free energy
$\Delta G$, i.e.,

$$\Delta V = (\delta \Delta G / \delta P)_T .  \qquad (6)$$

For self-diffusion, this can be expressed by

$$\Delta V = -kT \left(\frac{\partial \ln D}{\partial P}\right)_T + kT\left[\left(\frac{\partial \ln a^2}{\partial P}\right)_T + \left(\frac{\partial \ln \nu}{\partial P}\right)_T\right] ,  \qquad (7)$$

where $a$ is the lattice parameter, and $\nu$ is the aver-
age atomic vibration frequency. Recently, it has
been shown[27] that, when $D$ is determined by means
of serial sectioning, the lattice parameter should
not be included. The variation of the average vi-
bration frequency with pressure can be estimated
by assuming $\nu$ to be the characteristic frequency
determined from the Lindemann relation. The sec-
ond term on the right-hand side of Eq. (7) is not
well known and, in the case of sodium, amounts to
a few % of $\Delta V$; since this is within the over-all ex-
perimental accuracy, it has been neglected. Values
of the activation volume (expressed as activation
volume relative to the atomic volume) and the per-
centage contribution of each process to diffusion at
the temperature stated are given in Table IV. In
order not to associate an activation energy or vol-
ume with a given process, the low-temperature
process is referred to in Table IV as (1) and the high
temperature as (2). The percentage contributions
are compared with those determined from Eq. (4).
A further comparison is made by determining the
activation volumes when the fit is made by holding
the percentages obtained from Eq. (4) as fixed pa-
rameters. Table IV shows that at 14.8 °C, $\frac{2}{3}$ of the
diffusion occurs by a process having a relative ac-
tivation volume of approximately 0.3 and that the
relative activation volume for the other process is
approximately 0.7. At 91.3 °C, the relative activa-
tion volumes appear to be approximately the same
but, at this temperature, two-thirds of the diffusion
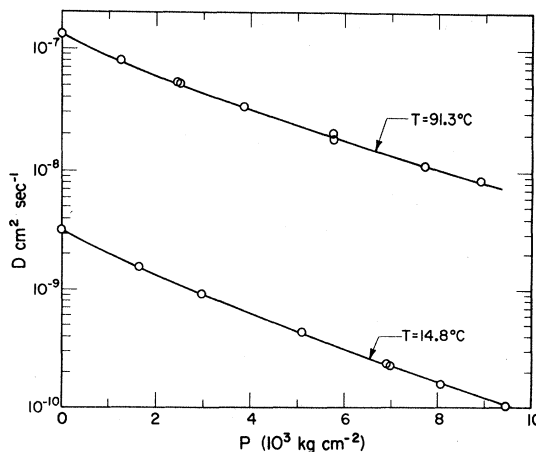occurs by a process having the relative activation



FIG. 3. Diffusion of $^{22}$Na in sodium as a function of
pressure.

TABLE IV. Percentage of diffusion process at 14.8 and 91.3 °C, with the relative activation volume of each process determined for a two-exponential fit.

| Temperature (°C) | Percentage (2) | $\Delta V_2/V$ | Percentage (1) | $\Delta V_1/V$ | Remarks |
|---|---|---|---|---|---|
| 14.8 | $35 \pm 1$ | $0.77 \pm 0.04$ | $65 \pm 1$ | $0.33 \pm 0.02$ | Floating |
| 91.3 | $66 \pm 2$ | $0.66 \pm 0.02$ | $34 \pm 1$ | $0.26 \pm 0.06$ | concentration |
| 14.8 | 41 | $\circ \circ \bullet$ | 59 | $\circ \bullet \bullet$ | From Eq. (4) |
| 91.3 | 67 | $\circ \circ \bullet$ | 33 | $\circ \circ \bullet$ | |
| 14.8 | 41 | $0.69 \pm 0.03$ | 59 | $0.32 \pm 0.01$ | Fixed |
| 91.3 | 67 | $0.65 \pm 0.02$ | 33 | $0.26 \pm 0.07$ | concentration |

volume of 0.7. As can be noted, fixing the percentages of the two processes determined from Eq. (4) does not appreciably alter the activation volumes.

The three-exponential fit to the pressure data is given in Table V in terms of the activation volume of each process and the percentage contribution of each process to diffusion at ambient pressure. The 14.8 °C isotherm data suggest that diffusion at this temperature can be accounted for by the two lower-temperature processes. The 91.3 °C isotherm data also imply that if three processes operate at this temperature, then the upper two have very similar activation volumes.

The evidence from both the temperature and pressure data strongly suggests that at 14.8 °C and ambient pressure about two-thirds of the diffusion occurs by means of the low-temperature process. The process has an activation energy of approximately 8700 kcal and a relative activation volume of 0.3. At 91.3 °C, approximately 40% of the diffusion occurs by the low-temperature process. Also, if two high-temperature processes are present, then apparently they have similar activation volumes. The relative activation volume of this process or processes is approximately 0.7.

### C. Entropy of Activation

The entropy of activation associated with each process can be determined from the values of $D_0$ in Eqs. (4) and (5). Values of the entropy $\Delta S$ were obtained from the equation

$$D_0 = \gamma a^2 \nu f e^{\Delta S/k} , \qquad (8)$$

where $\gamma$ is a geometrical constant that depends on the unit-cell geometry and the assumed jump mechanism, and $\nu$ is an average atomic vibration frequency. A major problem involves assigning a value for $\nu$ recognizing that a value assumed for a vacancy mechanism might be expected to be too low for an interstitial mechanism and too high for a divacancy mechanism. The values $\gamma$ and $f$ also change with mechanism but these values are known for the most common mechanisms. To calculate the entropies, the values used were the same in all cases: $\gamma = 1$, $f = 0.727$, and $\nu = 3.33 \times 10^{12}$ sec$^{-1}$. This vibration frequency is the characteristic lattice frequency determined for sodium assuming a Debye temperature of 159 °K. From Eq. (4), the entropies are

$$\Delta S_1 = 0.25k, \quad \Delta S_2 = 5.1k ;$$

and from Eq. (5), the entropies are

$$\Delta S_1 = 0.7k, \quad \Delta S_2 = 3.5k, \quad \text{and} \quad \Delta S_3 = 7.5k ,$$

where the subscripts are the same as used in Tables IV and V.

### D. Diffusion as a Function of Temperature at 7000 kg cm$^{-2}$

Measurements of the diffusion coefficient at 7000 kg cm$^{-2}$ were made as a function of temperature from 14.8 to 117.1 °C, and the values are tabulated in the first three columns of Table VI. Al-

TABLE V. Percentage of diffusion process at 14.8 and 91.3 °C, with the relative activation volume of each process determined for a three-exponential fit.

| Temperature (°C) | Percentage (3) | $\Delta V_3/V$ | Percentage (2) | $\Delta V_2/V$ | Percentage (1) | $\Delta V_1/V$ | Remarks |
|---|---|---|---|---|---|---|---|
| 14.8 | $7 \pm 2$ | $0.70 \pm 0.02$ | $29 \pm 1$ | $0.76 \pm 0.07$ | $64 \pm 2$ | $0.33 \pm 0.01$ | Floating concentration |
| 91.3 | 28 | $0.68 \pm 0.21$ | 36 | $0.68 \pm 0.25$ | 41 | $0.27 \pm 0.10$ | |
| 14.8 | 7 | $\circ \circ \bullet$ | 26 | $\bullet \bullet \circ$ | 67 | $\bullet \bullet \bullet$ | From Eq. (5) |
| 91.3 | 27 | $\bullet \bullet \circ$ | 34 | $\bullet \bullet \bullet$ | 39 | $\circ \bullet \bullet$ | |

TABLE VI. Diffusion of $^{22}$Na and $^{24}$Na in sodium at 7000 kg cm$^{-2}$ as a function of temperature.

| Temperature (°C) | Pressure (kg cm$^{-2}$) | $D$ (cm$^2$ sec$^{-1}$) | $\left(\dfrac{D_{22}}{D_{24}} - 1\right)$ | $D$(cm$^2$ sec$^{-1}$) (7000 kg cm$^{-2}$) |
|---|---|---|---|---|
| 117.1 | 6862 | $4.23 \pm 0.01 \times 10^{-8}$ | $0.0118 \pm 0.0003$ | $4.06 \pm 0.01 \times 10^{-8}$ |
| 94.9 | 7129 | $1.69 \pm 0.01 \times 10^{-8}$ | $0.0133 \pm 0.0004$ | $1.76 \pm 0.01 \times 10^{-8}$ |
| 94.6 | 7614 | $1.38 \pm 0.01 \times 10^{-8}$ | $0.0126 \pm 0.0003$ | $1.68 \pm 0.01 \times 10^{-8}$ |
| 80.7 | 6954 | $9.09 \pm 0.06 \times 10^{-9}$ | $0.0149 \pm 0.0002$ | $8.95 \pm 0.06 \times 10^{-9}$ |
| 78.8 | 6932 | $8.60 \pm 0.04 \times 10^{-9}$ | $0.0149 \pm 0.0002$ | $8.42 \pm 0.04 \times 10^{-9}$ |
| 60.5 | 7242 | $3.20 \pm 0.03 \times 10^{-9}$ | $0.0153 \pm 0.0010$ | $3.47 \pm 0.03 \times 10^{-9}$ |
| 40.7 | 7207 | $1.10 \pm 0.01 \times 10^{-9}$ [a] | $0.0157 \pm 0.0010$ [a] | $1.19 \pm 0.01 \times 10^{-9}$ [a] |
| 14.8 | 6889 | $2.39 \pm 0.01 \times 10^{-10}$ | $0.0179 \pm 0.0004$ | $2.30 \pm 0.01 \times 10^{-10}$ |

[a]Values have been corrected for "cusping."

though allowance was always made for the increase of pressure when heating the high-pressure vessel, it was not always possible to reproduce exactly the same conditions, and so the pressures vary as shown in column 2 of Table VI. The data of Table III were used to correct the values of $D$ to a pressure of 7000 kg cm$^{-2}$ and these values are given in the last column of Table VI and plotted in Fig. 4. The values at 40.7 °C have been corrected for "cusping." The correction was $-4\%$ on the diffusion coefficient and $+8\%$ on the isotope effect. The data of Nachtrieb et al.[20] for 8000 kg cm$^{-2}$ and the present ambient-pressure data are also plotted in Fig. 4. Nachtrieb's data are in good agreement with the present work but the scatter does not allow for conclusions concerning the "straightness" of the Arrhenius line. The 7000 kg cm$^{-2}$ isobar shows no curvature, in contrast to the ambient-pressure data. As noted earlier over the measured temperature range at 7000 kg cm$^{-2}$, the majority of diffusion occurs by means of the low-temperature process, and, for any one mechanism, a curvature in the
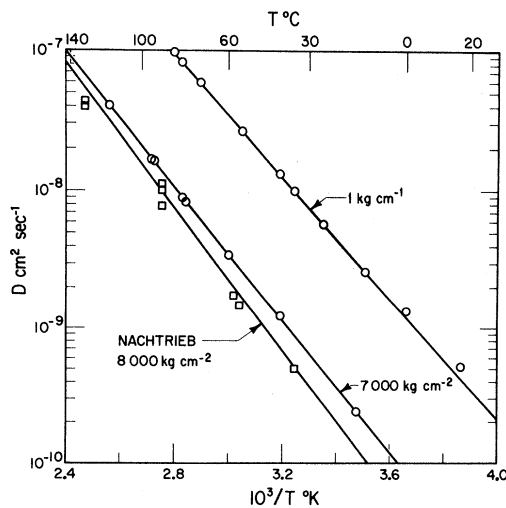
Arrhenius line would not be expected. The least-squares fit to the data of Table VI gives

$$D = 0.085 \pm 0.003\, e^{-(11270 \pm 60)/kT} . \qquad (9)$$

### E. Isotope Effect

The $^{24}$Na and $^{22}$Na isotopes were diffused simultaneously into the sodium sample. The ratio of the specific activities $(C_{22}/C_{24})$ as a function of penetration (i.e., $C_{22}$) has been shown,[28] using Eq. (2), to be

$$\ln\left(\frac{C_{22}}{C_{24}}\right) = \text{const} - \ln C_{22}\left(\frac{D_{22}}{D_{24}} - 1\right), \qquad (10)$$

where the subscripts 24 and 22 refer to the isotopes $^{24}$Na and $^{22}$Na, respectively. Examples of the experimental plots $\ln C_{22}/C_{24}$ vs $\ln C_{22}$ are shown in Fig. 5. These particular plots are from the same experiments as the concentration profiles shown in Fig. 1 and show the apparent lack of effect of a pressure of 7000 kg cm$^{-2}$ on the isotope effect at 79 °C. Since the effect of pressure on the isotope effect was very small, the accuracy of the previous data at ambient pressure had to be improved. The present data are tabulated with their individual er-
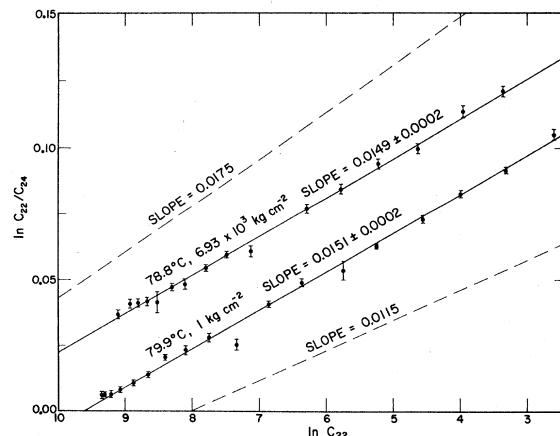


FIG. 4. Diffusion of $^{22}$Na in sodium as a function of temperature at different pressures.



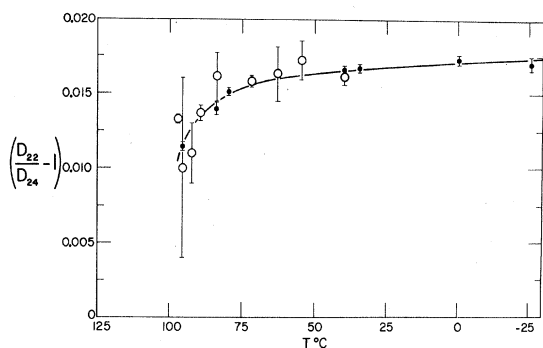FIG. 5. Diffusion of $^{22}$Na and $^{24}$Na in sodium.

FIG. 6. Variation of $(D_{22}/D_{24} - 1)$ with temperature at ambient pressure; ■, data from Ref. 14; ●, present work.

rors in Table II and plotted with the data of Ref. 14 in Fig. 6. The minimum and maximum values found for the isotope effect as a function of temperature have been shown as slopes in Fig. 5.

The data of Ref. 14 were interpreted as showing a constant value of 0.016 for the isotope effect over the temperature range 40–84 °C, but above 84 °C there was a decrease in value to 0.013 at the melting point. This premelting phenomena was attributed to local melting at dislocations caused by the segregation of potassium to these dislocations. However, the sodium used in this work had a potassium impurity level of at least two orders of magnitude lower than the sodium previously used. As can be seen in Fig. 6, the present data and the earlier work are in good agreement. The smaller error in the present data defines a line showing that the isotope effect decreases as the temperature increases over the entire temperature range, with a more rapid decrease in value as the melting point is approached.

At this point it became obvious that measurements of the variation of the isotope effect with pressure at a given temperature would be less valuable than measurements at a fixed pressure as a function of temperature. The measurements of the diffusion coefficients as a function of pressure showed that, as the pressure increased, the percentage of diffusion occurring by the low process increased until (above 7000 kg cm$^{-2}$) the majority of the diffusion occurred by the one process. Values of the isotope effect were obtained at a pressure of 7000 kg cm$^{-2}$ over the temperature range 14.8–117.1 °C and are given in Table VI and plotted in Fig. 7. The solid line in Fig. 7 has been drawn through the ambient-pressure data of Fig. 6. The dashed line indicates the best line through the high-pressure data. At two of the higher temperatures, the experiments were repeated to check the reproducibility of the data. Within experimental error, the data reproduced well and confirmed that over

much of the temperature range a pressure of 7000 kg cm$^{-2}$ causes little change in the value of the isotope effect.

## IV. DISCUSSION

### A. Mechanisms of Diffusion

Although the present work has yielded considerable information, it is not sufficient to make unambiguous identification of the diffusion processes in sodium. There is a considerable amount of experimental and theoretical information pertaining to the problem of diffusion in sodium. However, all the available information has not solved the problem, and a discussion of all the possible explanations of the present data is appropriate in an attempt to distinguish the most likely diffusion processes. From the presentation of the results, at least two processes apparently must be taken into account, but, for the sake of completeness, one-, two-, and three-mechanism models of diffusion will be discussed.

### B. One-Mechanism Models

A number of interpretations of the data can be made on the basis of a one-mechanism model. Three possibilities will be discussed.

(i) When diffusion data are found to obey the linear Arrhenius relation given by Eq. (3), strong evidence exists that one mechanism is operating over the entire temperature range. Deviations from linearity of the Arrhenius line have frequently been considered as an indication that more than one process is operative. In recent years,[29-32] the inherent curvature of the Arrhenius plot in diffusion experiments has been considered. Nowick and Dienes[31] showed that the temperature dependence of the activation energy is given by

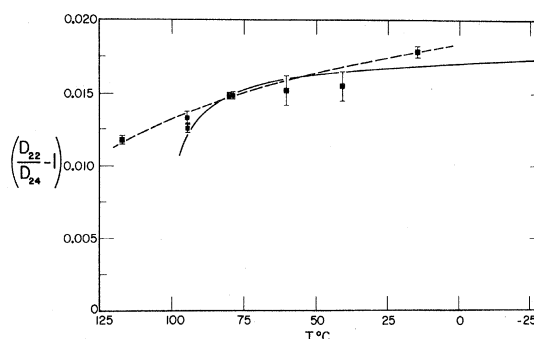$$\frac{dQ}{dT} \equiv B = \Delta Cp \ , \tag{11}$$



FIG. 7. Variation of $(D_{22}/D_{24} - 1)$ with temperature at 7000 kg cm$^{-2}$. The solid line has been drawn through the ambient-pressure data of Fig. 6. The dashed line indicates the best line through the high-pressure data.

where $\Delta C_p$ is the difference in specific heat of the material containing an activated vacancy and that of the perfect lattice. Estimates of $B$ show that $B \lesssim k$, the gas constant. The present data yield a value of $B$ equal to $5k$; thus, the temperature dependence of $Q$ is too great to be accounted for by the Nowick and Dienes model.

(ii) Previous discussions of experimental data pertaining to diffusion in sodium or other bcc metals have concentrated on a one-mechanism model, which is equally true for most of the theoretical approaches. Because these discussions and approaches fit more clearly with the processes discussed in the next sections, they will not be referred to here. However, one recent theoretical approach[33] that has been applied to $\alpha$-Fe could give an explanation for much of the observed data.

Tsai et al.,[33] have applied a molecular dynamic type of calculation to the motion of interstitials and vacancies in a crystalline lattice. The authors found that the single-vacancy migration energy calculated from the dynamical model was lower than that from static calculations. The explanation for this discrepancy was in terms of the double-peaked potential barrier to vacancy motion. Under dynamic conditions, the barrier fluctuates in height, but because of the presence of the vacancy the amplitude of the fluctuations for each of the peaks will be different. In the event that the first part of the barrier has larger fluctuations than the second part, a migrating atom could move past the first barrier at a low part of the cycle and then receive additional energy as the first barrier rose to help the atom past the second barrier. This "pumping" action is purely a qualitative argument to explain the lower value of the migration energy obtained from the dynamical calculations of Tsai et al.

Assuming the "pumping" model has some validity, Peterson[34] has suggested how it may explain the present results. The pumping action could be expected to increase as the temperature increases leading to a positive curvature in the $\ln D$-vs-$1/T$ plot. In a similar manner, an increase in pressure should decrease the pumping action and cause positive curvature in the $\ln D$-vs-pressure plot. As the temperature is increased, there could be an increase in the interaction between the jumping atom and the barrier atoms as a direct result of the increase in pumping action. This would result in a smaller $\Delta K$ and a lowering of the isotope effect with increasing temperature. Thus a qualitative explanation of the observed data is possible but before a reasonable assessment of the merit of this "pumping action" model can be made, a considerable amount of calculation will be required.

(iii) In the present commonly accepted theory of diffusion, the crystal lattice is considered to be made up of atoms behaving as simple harmonic oscillators. Anharmonic effects are not usually considered when discussing diffusion data. However, recent work by Flynn[35] suggests that some of the curvature found in the Arrhenius plots of diffusion data could be accounted for by anharmonicity.

### C. Two-Mechanism Models

The present data can be analyzed in terms of two diffusion processes giving activation energies of 11.5 and 8.5 kcal/mole [Eq. (4)] and relative activation volumes of 0.7 and 0.3, respectively (Table IV). Before considering what type of mechanism one should associate with each of these processes, the experimental values and theoretical calculations pertaining to self-diffusion in sodium will be discussed.

The standard interpretation of self-diffusion is made in terms of Eq. (4), where

$$D_0 = f \gamma a^2 \nu e^{(S_f + S_M)/k} \qquad (12)$$

and

$$Q = E_f + E_m . \qquad (13)$$

The separate terms for the energy of formation $E_f$ and the energy of migration $E_m$ have been determined by a number of techniques. Values of $E_f$ have been determined by measurements of electrical resistivity,[36] specific heat,[37,38] and by careful measurements of the macroscopic change in length and x-ray lattice parameter as a function of temperature.[39,40] These values and the theoretical calculations[41,42] are listed in Table VII. On the basis of these numbers and the self-diffusion data for sodium,[14,43] the conclusion was made that 95% of the activation energy for diffusion was formed from the energy of formation. This conclusion followed closely the suggestion by Fumi that the energy of motion should be small.

Measurements of electrical resistivity can be used for determination of $E_f$; however, they suffer from two disadvantages: (a) the effect of a unit concentration of point defects is unknown; and (b) one has no measure of the "ideal" or defect-free crystal. This makes for considerable error in this type of measurement. The specific-heat measurements only suffer from the second of the above disadvantages. As Martin notes in his second paper, the net vacancy concentration at the melting point is considerably higher than expected, but that this could indicate interstitial defect formation. The theoretical calculations of Fumi have been repeated by Shyu[44] who used a more realistic potential and, allowing for relaxation, determined a value of 8.1 kcal/mole for the vacancy formation energy. Thus, the evidence that the energy of formation is a large fraction of the activation energy is not necessarily borne out by any of the above data, with the exception of that of Feder and Charbnau.[40] Sullivan

TABLE VII.  Values of the single-vacancy formation energy.

| $E_F$ (kcal/mole) | Method | Refs. |
|---|---|---|
| 9.1 | Electrical resistivity | 36 |
| (10.5)8.2 | Specific heat | 37 and 38 |
| 3.2 | $\Delta l/l - \Delta a/a$ | 39 |
| 9.7 | $\Delta l/l - \Delta a/a$ | 40 |
| 12.2 | Theoret calc | 41 |
| 10.6 | Theoret calc | 42 |
| 8.2 | Theoret calc | 44 |

and Weymouth[39] made similar measurements but their data appear to be less accurate. We wish, therefore, to analyze the present data in conjunction with that of Feder and Charbnau but without the frequently made assumption that $E_f = 0.95Q$ for bcc sodium. A number of combinations of defect mechanisms could be considered at this point. In the interest of simplicity, this discussion will follow the combinations of vacancies and interstitials, and divacancies and vacancies as examined by Feder and Charbnau in their analysis.

### 1. Vacancy and Interstitial Mechanisms

When Feder and Charbnau analyzed their data in terms of the two mechanisms, vacancy and interstitial, they obtained values for the energy and entropy terms as follows:

$$E_f^{1V} = 6.45 \text{ kcal/mole}, \quad E_f^i = 4.60 \text{ kcal/mole} ,$$

$$S_f^{1V} = 2.0 \text{ k} , \qquad S_f^i = -1.0 \text{ k} .$$

It would be equally appropriate with the present results to consider that the interstitials are responsible for the low-temperature process, since this process has the smaller activation volume. Some of the advantages of associating the two processes with a vacancy mechanism at high temperatures and interstitials at lower temperatures are as follows.

(a) The energy of vacancy formation is then 0.56 of the activation energy for diffusion. Values of the ratio $E_f^{1V}/Q$ for the fcc metals Cu, Ag, Au, and Al are in the range 0.54–0.63. If, on the other hand, the low process was chosen as the vacancy process, the $E_f^{1V}/Q > 0.95$. Recent work by Feder,[45] comparing measurements of the macroscopic change in length and x-ray lattice parameter as a function of temperature for lithium, shows that $E_f^{1V}/Q = 0.62$. It should be pointed out that the self-diffusion data for lithium[46–50] have shown very little curvature. However, any one set of experimental

data on lithium has not been measured over as wide a temperature range as the present sodium measurements.

(b) A negative entropy of formation for an interstitial is to be expected, as pointed out by Feder and Charbnau. The present breakdown of results, however, does indicate a positive entropy for vacancy migration and clears up the problem of a negative entropy found in the earlier interpretation.[40]

(c) The activation energy of diffusion has been correlated with the melting temperature ($T_m$) and with the latent heat of melting ($L_m$).[22] These correlations are given in Table VIII. The alkali metals appear to fall into a very close pattern. The diffusion coefficients in sodium have been measured to much lower relative temperatues than the other alkali metals. The low-temperature process in sodium would predominate only at low relative temperatures. Thus, if the value 8.5 kcal/mole is used, it is not surprising that the ratios $Q/T_m = 23.0$ and $Q/L_m = 13.7$ no longer fall in line with the other data. Although these correlations do not aid in identification of the mechanisms, they do suggest that, at high relative temperatures, the mechanism of diffusion is the same in each alkali metal.

The variation of the isotope effect with temperature remains to be explained. Assuming that the value of $\Delta K$ does not vary with pressure or temperature, then one would expect the temperature variation of the isotope effect to follow an equation of the form

$$[(D_{22}/D_{24}) - 1] = \sum_i p_i f_i \Delta K_i \Delta m_i , \qquad (14)$$

where the terms other than $p$, the percentage of the diffusion occurring by that mechanism, have been previously defined and the subscript $i$ refers to the $i$th mechanism. The mass term has been written as $\Delta m_i$, since this will be a function of the masses of all the atoms involved in the jump process. From the two-exponential fit to the diffusion data, one can obtain values of $p_i$ and, by the judicial choice of mechanisms, values of $f_i$ and $\Delta m_i$ can be ascertained.

Equation (14) was used to obtain a series of simultaneous equations that can be used to find the strength of the isotope effect $f\Delta K$ for each mechanism. It became immediately obvious that by using

TABLE VIII.  Melting-point correlation for alkali metals.

| Element | $T_m$ (°K) | $Q$ (kcal/mole) | $L_m$ (cal) | $Q/T_m$ | $Q/L_m$ |
|---|---|---|---|---|---|
| Li | 453.7 | 12.87 | 714.8 | 28.4 | 18.0 |
| Na | 371.0 | 11.50 | 621.7 | 31.0 | 18.5 |
| K | 336.4 | 9.75 | 559.1 | 29.0 | 17.4 |
| Rb | 312.6 | 9.40 | 521.4 | 30.1 | 18.0 |

discrete values of $\Delta K_i$ it was not possible for Eq. (14) to describe the observed data if only two simple processes such as vacancy and interstitial were considered.

### 2. Divacancy and Vacancy Mechanisms

Seeger[51] has pointed out that it would be possible to associate the first process with vacancies and the second and third with divacancies. Two types of divacancies are possible, nearest-neighbor vacant sites and next-nearest-neighbor vacant sites. The binding energies for these divacancies have been calculated for $\alpha$-Fe [52,53] and depending upon the interaction potential chosen, either type could be the more stable. To explain the present data, Seeger suggests that the relative amounts of diffusion occurring by either type of divacancy will vary with temperature. Thus, different correlation factors for the different divacancy jump processes will lead to an apparent variation of the correlation factor with temperature. This explanation has the advantage that it could explain the variation of diffusion coefficient and isotope effect with temperature. The results show that the activation volume for processes two and three are essentially the same and this could also be expected for the two types of divacancy. This type of analysis overcomes the problem of associating $\Delta K < 1$ for interstitial motion. $(\Delta V/V)_1$ is approximately 43% of $(\Delta V/V)_2$ and this would appear reasonable; however, if one anticipates greater relaxation around a divacancy, a value greater than 50% would be expected.

When Feder and Charbnau analyzed their data to consider the divacancy and vacancy defects, they found that by making the binding entropy large and negative the divacancy contribution could be raised to at most 40% of the total concentration. Even for these conditions the values of $E_f^{1V} = 9.0$ kcal/mole and $S_f^{1V} = 4.5k$ are quite high. It is interesting to note that, if one assumes that the low process is that of a vacancy mechanism, $E_f^{1V}$ is greater than the activation energy for the low process ($Q = 8.5$ kcal/mole). However the data of Feder and Charbnau should be reanalyzed in the light of the present work, and further discussion of the divacancy-vacancy model will be published by Seeger.

### D. Three-Mechanisms Model

The present data have been analyzed in terms of three mechanisms giving activation energies of 14.0, 10.8, and 8.7 kcal/mole [Eq. (6)] and relative activation volumes 0.7, 0.7, and 0.3, respectively (Table V). Equation (14) is used to probe the identification of these mechanisms. At 7000 kg cm$^{-2}$ and 14.8 °C, 98% of the diffusion occurs by the low-temperature process, thus the value of $f_1 \Delta K_1 \delta m_1$ is 0.018 at this point. At ambient pressure and 14.8 °C, we obtain

$$0.07\,f_3 \Delta K_3 \delta m_3 + 0.27\,f_2 \Delta K_2 \delta m_2$$

$$= 0.016 - 0.66 \times 0.018 , \tag{15}$$

and at ambient pressure and 91.3 °C, we obtain

$$0.24\,f_3 \Delta K_3 \delta m_3 + 0.36\,f_2 \Delta K_2 \delta m_2$$

$$= 0.013 - 0.4 \times 0.018 . \tag{16}$$

Solving Eqs. (15) and (16), we obtain

$$f_3 \Delta K_3 \delta m_3 = 0.003 , \quad f_2 \Delta K_2 \delta m_2 = 0.014 ,$$
$$f_1 \Delta K_1 \delta m_1 = 0.018 . \tag{17}$$

The errors for these values for processes one and two are at least $\pm 20\%$ and considerably greater for process three. The numbers in Eq. (17) serve to indicate the order of the values for the various processes. If, as we considered in the discussion of two-mechanism models, interstitials are the lowest process, the value obtained must be explained either in terms of an interstitial mechanism or interstitialcy mechanism. These mechanisms have been discussed.[14,54] In these discussions, pure interstitial diffusion was eliminated because of the small value of the isotope effect when taken in conjunction with the fact that all instances of interstitial diffusion so far investigated showed that inverse-root-mass relation was obeyed and $\Delta K \simeq 1$.[28] However, all the available data involved impurity diffusion where the size of the impurity ion is small in comparison with the space in the interstitial sites of the lattice. It is perhaps unwise to draw the conclusion that $\Delta K \simeq 1$ for self-diffusion by interstitials. For the simple interstitial mechanism and the value of $f_1 \Delta K_1 \delta m_1$ equal to 0.018, we have $\Delta K_1 = 0.40$.

The second process was assumed to be a vacancy mechanism. This would mean that for a value of $f_2 \Delta K_2 \delta m_2$ equal to 0.014 we have $\Delta K_2 = 0.38$. This is a very low value and appears to destroy any connection between $\Delta K$ and $\Delta V/V$. This connection was established for metals where diffusion was thought to occur by a vacancy mechanism. The present work indicates that a close examination of both $\Delta K$ and $\Delta V/V$ fail to show any connection between these parameters for any of the simple mechanisms we have chosen to discuss. It should be mentioned that the calculations of $\Delta K$ for a vacancy mechanism in sodium, Huntington et al.,[55] and Brown et al.,[56] have shown that $\Delta K \simeq 1$. Recent calculations by Achar,[57] using the dynamical theory of Rice[58] and Flynn,[59] have shown that $\Delta K \simeq 0.5$ for a vacancy mechanism.

The value of $f_3 \Delta K_3 \delta m_3 = 0.003$ for the high-temperature process has to be explained. This is indeed a very low value and one wonders if an activation state theory is applicable in this case. Since

both $\Delta K$ and $\delta m$ are terms that apportion the number of atoms taking part in the jump, it would seem more appropriate to put

$$\left(\frac{(n-1)m_0 + m_\alpha}{(n-1)m_0 + m_\beta}\right)^{1/2}$$

equal to the measured value of $f_3 \Delta K_3 \delta m_3$ and determine the number of atoms $n$ taking part in the jump process. If this procedure is followed, $n > 20$. Cocking[60] has found, from neutron diffraction experiments on liquid sodium just above the melting point, that about 30 atoms appear to be cooperating in the jump process. Considering the rather large error that must be attributed to $f_3 \Delta K_3 \delta m_3$, the two numbers are not significantly different. Calculations have shown[42] that in sodium the relaxation around a vacancy is appreciable and extends over several shells of neighbors. As the melting temperature is approached and the vacancy concentration increases, the relaxation around any given vacancy could affect that around another vacancy. These interactions could establish regions of the crystal where diffusion occurs by a multiatom process. The diffusion activation energy is the sum of a formation and motion term and could be higher than that for a single vacancy, as observed experimentally. The activation volume for this multiatom process could be expected to be similar or slightly smaller than the activation volume for a single vacancy. As the vacancy concentration increases with temperature, more and more interaction occurs causing a rapid decrease in the measured value of the isotope effect. The rapid decrease in the isotope effect is not observed with the measurements at 7000 kg cm$^{-2}$. However, the melting temperature of sodium at this pressure is approximately 145 °C, therefore, the vacancy concentration may not be sufficient for appreciable interaction.

The possibility of an interstitial mechanism has been considered in the discussion of two- and three-mechanism models. It should be emphasized that although computer simulation of some alkali-metal diffusion[56,61] has suggested the possibility of interstitials, no definite experimental evidence has been found. To clarify whether interstitials could be responsible for the low-temperature process, the effect of solvent additions to the self-diffusion coefficient will be investigated in both the high- and low-temperature range. At low temperature ($\sim 200$ °K) it should be possible to make NMR measurements on single crystals of sodium and determine the order parameter defined by Ailion and Ho.[62] Determination of this order parameter could establish whether interstitials are the predominant defect.

### E. Previous Activation Volume Data

Measurements of the effect of pressure on the self-diffusion of sodium[20] showed that at 90 °C, $\ln D$ did not vary linearly with pressure. The Kohler and Ruoff[63] suggestion that the data of Ref. 20 could be equally well represented by a linear fit, has not been borne out by the present work. The data of Ref. 20 agrees with the 91.3 °C isotherm of the present work within experimental error. Nachtrieb et al. interpreted their data as a decrease of the activation volume with pressure. This variation of activation volume fitted reasonably well with an equation for the activation volume derived from the Clausius-Clapeyron equation. It is not clear why the activation volume should be related to the melting temperature in any rigorous way, and the present explanation of two or more processes with different activation volumes appears to be more satisfactory. The measurements of the effect of pressure on the NMR line narrowing in both lithium and sodium have been made by Hultsch and Barnes.[50] They obtained a value of $\Delta V/V = 0.41$ for sodium and concluded that this was to be expected since it agreed with the value obtained from the melting-point correlation of Rice and Nachtrieb.[64] Our present work allows one to calculate at $\sim 225$ °K (temperature at which the NMR measurements were made) that at least 85% of the diffusion was by the low-temperature process. Measurements were made between 1 and 3500 kg cm$^{-2}$. The slope found from the data can be interpreted as being largely due to an activation volume of the low process ($\Delta V/V = 0.3$) but, since the pressure range was not large enough, the contribution from the high-temperature process ($\Delta V/V = 0.7$) raised the measured value of $\Delta V/V$ to only 0.41.

The above explanation suggests that in materials where two diffusion processes are known to be operative a curvature should be observed in the $\ln D$-vs-$P$ plot. One example is the recent work on silver,[5,13] which showed that as the melting temperature is approached an appreciable fraction of the diffusion occurs by means of divacancies. Measurements of the effect of pressure on the self-diffusion rate in silver at 900 °C have been made[16,65] but no curvature was observed. At 900 °C and ambient pressure, the analysis of Mehrer and Seeger[13] shows that half of the diffusion occurs by means of divacancies. With this parameter and the assumption that the divacancy activation volume ($\Delta V_D$) is twice the vacancy activation volume ($\Delta V_V$), one can fit a calculated $\ln D$-vs-pressure curve to the experimental data. A good fit is obtained with $\Delta V_D/V = 1.2$ and $\Delta V_V/V = 0.6$, which appear to be reasonable values. The higher values of $\Delta V/V$ for silver lead to a far smaller amount of curvature in the $\ln D$-vs-pressure curve than the curvature found for sodium. To obtain curvature similar to that for sodium, the pressure data would have to be extended to approximately 30 000 kg cm$^{-2}$. Thus
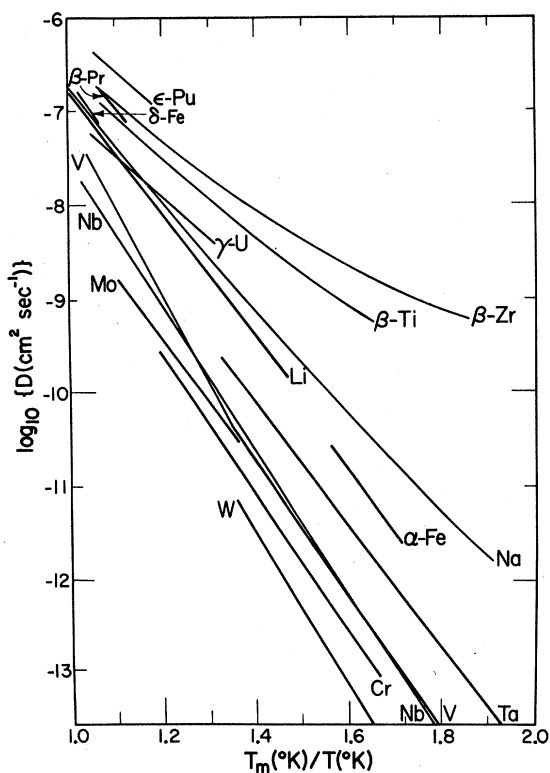
FIG. 8. Comparison of self-diffusion rates of bcc metals on a relative temperature scale.

### F. Normal vs Anomalous bcc Diffusers

Previous reviews[22] of diffusion in bcc metals contain much discussion of "normal" and "anomalous" diffusion. At first glance one could expect to find differences in the diffusion behavior of close-packed fcc and hcp metals from the behavior in the more open structure of bcc metals. In the past it was the similarities of the "normal" bcc diffusers that were noted, and discussion centered around explaining the results found in the anomalous metals. If all the diffusion data for bcc metals is plotted using a normalized temperature scale (Fig. 8), the alkali metals appear more as "anomalous" rather than "normal" diffusers.

The data on self-diffusion in lithium show no curvature, although it might be noted that the most recent and careful NMR data,[48] measured over the temperature range 110–80 °C, show a lower activation energy (11.8 kcal) than the tracer diffusion data (35–170 °C) with an activation energy of 12.8 kcal. Since the Debye temperature (62 °C) is high relative to the temperature of diffusion measurements, the data might be expected to be affected by

quantum effects and any possible curvature due to different mechanisms could be masked.

When normalizing plots to $T_m/T$, it is interesting to compare the only available data on isotope effects in bcc metals. Using values of $\delta m_i$ for a single-atom jump process, the values of $f\Delta K$ for sodium and bcc iron[10] are compared in Table IX. Although the data for $\alpha$-Fe has a large error due to experimental difficulties, it is interesting that the values for $\delta$-Fe agree very well with those of sodium. Since isotope-effect measurements are very much more sensitive to the concentrations of, and the differences between, the various atomic processes, the agreement between $\delta$-Fe and Na is perhaps significant. The implication is strong that given sufficiently accurate measurements one would no longer be able to divide bcc metals into two subgroups, normal and anomalous. It may be that further careful investigation will show that the open structure of bcc metals allow several mechanisms to be operative at the same temperature. This is of course speculation, however 10 years ago it was not anticipated that the effect of divacancies on diffusion in fcc metals would be either appreciable or, from self-diffusion measurements, measurable.

Neumann[66] has discussed the diffusion data for bcc metals in terms of divacancies and vacancies. Although analyses of this type are extremely difficult, it is noteworthy that in very few bcc metals do the data truly justify the consideration of only one mechanism. As Peterson has stated,[67] the definitions of "normal" and "anomalous" metals may change during the coming years and isotope-effect experiments and measurements of activation volume on a number of the bcc metals would help considerably in clarifying the diffusion behavior in bcc metals.

### V. CONCLUSIONS

Analysis of all the present data strongly suggests that over the measured temperature range, three processes are responsible for diffusion in sodium. The activation energies are 14.0, 10.8, and 8.7 kcal/mole, with the latter activation energy most firmly established. The relative activation volumes

TABLE IX. Comparison of isotope effects for iron and sodium.

| $T_m(°K)/T(°K)$ | Iron    $f\Delta K$ | Sodium |
|---|---|---|
| 1.043 | $0.333 \pm 0.007$ | 0.329 |
| 1.060 | $0.338 \pm 0.005$ | 0.345 |
| 1.073 | $0.337 \pm 0.005$ | 0.351 |
| 1.074 | $0.339 \pm 0.005$ | 0.351 |
| 1.547 | $0.42 \pm 0.04$ | 0.394 |
| 1.548 | $0.46 \pm 0.04$ | 0.394 |

of the three processes are 0.7, 0.7, and 0.3, and, again, the lowest-temperature process has the more firmly established activation volume. On the basis of the present data, it is not possible to associate unambiguously a defect mechanism for each of these three processes. The proposal of interstitials, vacancies, and a multiatom process cannot be considered with confidence unless the experimental investigations mentioned in the discussion show evidence for an interstitial mechanism at low temperatures. The explanation of a vacancy mechanism at low temperatures and two sorts of divacancy at high temperatures, proposed by Seeger,[62]

gives a good qualitative explanation of the data. No definite conclusions can be made on this model or the "pumping" model until more quantitative calculations are made.

## ACKNOWLEDGMENTS

*Work performed under the auspices of the U. S. Atomic Energy Commission.

[1]A. H. Schoen, Phys. Rev. Letters 1, 138 (1958).

[2]K. Tharmalingham and A. B. Lidiard, Phil. Mag. 4, 899 (1959).

[3]J. G. Mullen, Phys. Rev. 121, 1649 (1961).

[4]N. L. Peterson and L. W. Barr (unpublished).

[5]S. J. Rothman, N. L. Peterson, and J. T. Robinson, Phys. Status Solidi 39, 635 (1970).

[6]S. J. Rothman and N. L. Peterson, Phys. Status Solidi 35, 305 (1969).

[7]N. L. Peterson, Phys. Rev. 136, A568 (1964).

[8]N. L. Peterson and S. J. Rothman, Phys. Rev. 163, 645 (1967).

[9]A. P. Batra, Phys. Rev. 159, 487 (1967).

[10]C. M. Walter and N. L. Peterson, Phys. Rev. 178, 922 (1969).

[11]T. Heumann and R. Imm, J. Phys. Chem. Solids 29, 1613 (1968).

[12]D. Graham, J. Appl. Phys. 40, 2386 (1969).

[13]H. Mehrer and A. Seeger, Phys. Status Solidi 39, 647 (1970).

[14]J. N. Mundy, L. W. Barr, and F. A. Smith, Phil. Mag. 14, 785 (1966).

[15]M. Beyeler and Y. Adda, J. Phys. (Paris) 29, 345 (1968).

[16]C. T. Tomizuka, Progress in Very High Pressure Research (Wiley, New York, 1961), p. 266.

[17]L. Chhabildas and H. M. Gilder, Proceedings of the Marstrand Conference on Atomic Transport in Solids and Liquids (Verlag Z. Naturforch., Tübingen, Germany, 1970).

[18]M. A. Norton and C. T. Tomizuka, Bull. Am. Phys. Soc. 15, 390 (1970).

[19]R. E. Hannemann, R. E. Ogilvie, and H. C. Gatos, Trans. AIME 233, 691 (1965).

[20]N. H. Nachtrieb, J. A. Weil, E. Catalano, and A. W. Lawson, J. Chem. Phys. 20, 1189 (1952).

[21]A. D. LeClaire, Phil. Mag. 14, 1271 (1966).

[22]L. W. Barr and J. N. Mundy, Diffusion in Body-Centered Cubic Metals (American Society of Metals, Metals Park, Ohio, 1965).

[23]C. M. Lederer, J. M. Hollander, and J. Perlman, Table of Isotopes (Wiley, New York, 1967), 6th ed.

[24]R. E. Hannemann and H. M. Strong, General Electric Research Report No. 64-RL-3725X, 1964 (unpublished).

[25]S. J. Rothman and N. L. Peterson, Phys. Rev. 154, 552 (1967).

[26]M. Gabriel, Argonne National Laboratory Report No. ANL-7495, 1968 (unpublished).

[27]R. N. Jeffery and D. Lazarus, J. Appl. Phys. 41, 3186 (1970).

[28]L. W. Barr and A. D. LeClaire, Proc. Brit. Ceram. Soc. 1, 109 (1964).

[29]L. M. Levinson and F. R. N. Nabarro, Acta Met. 15, 785 (1967).

[30]L. A. Girifalco, Scripta Met. 1, 5 (1967).

[31]A. S. Nowick and D. J. Dienes, Phys. Status Solidi 24, 461 (1967).

[32]A. Seeger and H. Mehrer, Vacancies and Interstitials in Metals (North-Holland, Amsterdam, 1969).

[33]D. H. Tsai, R. Bullough, and R. C. Perrin, AERE Report No. TR-396, 1970 (unpublished).

[34]N. L. Peterson (private communication).

[35]C. P. Flynn, Proceedings of the Marstrand Conference on Atomic Transport in Solids and Liquids (Verlag Z. Naturforsch., Tübingen, Germany, 1970).

[36]D. K. C. Macdonald, J. Chem. Phys. 21, 177 (1953).

[37]D. L. Martin, Lattice Dynamics (Pergamon, New York, 1964), p. 255.

[38]D. L. Martin, Phys. Rev. 154, 571 (1967).

[39]G. A. Sullivan and J. W. Weymouth, Phys. Rev. 136, A1141 (1964).

[40]R. Feder and H. P. Charbnau, Phys. Rev. 149, 464 (1966).

[41]F. G. Fumi, Phil. Mag. 46, 1007 (1955).

[42]W.-M Shyu, D. Brust, and F. G. Fumi, J. Phys. Chem. Solids 28, 717 (1967).

[43]N. H. Nachtrieb, E. Catalano, and J. A. Weil, J. Chem. Phys. 20, 1185 (1952).

[44]W.-M. Shyu (private communication).

[45]R. Feder, Phys. Rev. B 2, 828 (1970).

[46]D. F. Holcomb and R. E. Norberg, Phys. Rev. 98, 1074 (1955).

[47]A. N. Naumov and G. Ya. Ryskin, Zh. Tekhn. Fiz. 29, 189 (1959) [Soviet Phys. Tech. Phys. 4, 162 (1959)].

[48]D. C. Ailion and C. P. Slichter, Phys. Rev. 137, A235 (1965).

[49]A. Lodding, J. N. Mundy, and A. Ott, Phys. Status Solidi 38, 55 (1970).

[50]R. A. Hultsch and R. G. Barnes, Phys. Rev. 125, 1832 (1962).

[51]A. Seeger (private communication).

[52]H. M. Pak and M. Doyama, J. Fac. Eng. Univ. Tokyo 30, 111 (1969).

[53]R. A. Johnson, Phys. Rev. 134, A1329 (1964).

[54]L. W. Barr and J. N. Mundy, Diffusion in Body Centered Cubic Metals (American Society of Metals,

Metals Park, Ohio, 1965), p. 171.

[55]H. B. Huntington, M. D. Feit, and D. Lortz, Crystal Lattice Defects **1**, 193 (1970).

[56]R. C. Brown, J. Worster, N. H. March, R. C. Perrin, and R. Bullough, Atomic Energy Research of Europe Report No. TP-407, 1970 (unpublished).

[57]B. N. N. Achar, Phys. Rev. B **2**, 3848 (1970).

[58]S. A. Rice, Phys. Rev. **112**, 804 (1958).

[59]C. P. Flynn, Phys. Rev. **171**, 682 (1968).

[60]S. J. Cocking, J. Phys. C **2**, 2047 (1969).

[61]I. M. Torrens and M. Gerl, Phys. Rev. **187**, 912 (1969).

[62]D. C. Ailion and P. P. Ho, Phys. Rev. **168**, 662 (1968).

[63]C. R. Kohler and A. L. Ruoff, J. Appl. Phys. **36**, 2444 (1965).

[64]S. A. Rice and N. H. Nachtrieb, J. Chem. Phys. **31**, 139 (1959).

[65]M. Beyeler and Y. Adda, *Physics of Solids at High Pressures* (Academic, New York, 1965), p. 349.

[66]G. M. Neumann, *Proceedings of the Thomas Graham Memorial Symposium* (Gordon and Breach, New York, 1969).

[67]N. L. Peterson, *Solid State Physics* (Academic, New York, 1968), Vol. 22, p. 409.

---

# Self-Diffusion in Potassium[†]

J. N. Mundy, T. E. Miller,[*] and R. J. Porte[‡]

*Argonne National Laboratory, Argonne, Illinois 60439*

(Received 23 November 1970)

The self-diffusion of $^{42}K$ in potassium has been measured over the temperature range $-52.2 \pm +61.8°$ C. The temperature dependence of the diffusion coefficient can be described by $D = 0.16 \pm 0.01\ e^{-(9360 \pm 50)/RT}$. However the deviations of the individual points from this Arrhenius line suggest that diffusion could be occurring by two mechanisms.

## INTRODUCTION

Metals with a bcc structure have been subdivided into two groups on the basis of their diffusional behavior.[1] The first or "normal" group contains Li, Na, K, Fe, Nb, Mo, Ta, and W. These metals have diffusion coefficients that obey the Arrhenius relation

$$D = D_0 e^{-Q/RT} . \qquad (1)$$

The preexponential factors for these metals lie between 0.1 and 10 $cm^2 sec^{-1}$, and the activation energies $Q$ obey the melting-point rule $Q = 32 T_m$ ($T_m$ is the melting point). The second or "anomalous" group contain $\beta$-Zr, $\beta$-Ti, $\beta$-Hf, V, Cr, $\gamma$-U, and $\epsilon$-Pu. These metals have diffusion coefficients that follow curved Arrhenius plots or have values of $D_0$ and $Q$ not in accordance with the above empirical rules.

Recent measurements of self-diffusion in sodium[2] have shown that when the experiments extended over a wide range of temperature, the diffusion coefficients followed a curved Arrhenius plot. The data could be fitted to a two-exponential equation of the form

$$D = D_{01} e^{-Q_1/RT} + D_{02} e^{-Q_2/RT} . \qquad (2)$$

The values of $D_{01}$ and $Q_1$ obtained are in accordance with the empirical rules for "normal" diffusion.

A close examination of the data on diffusion in bcc metals[2] indicates that not only does sodium not fit into the so-called "normal" group but that the concept of "normal" and "anomalous" bcc diffusers may be misleading. Measurements of the self-diffusion coefficient of potassium over a wide range of temperature were made to determine if the Arrhenius plot is truly linear. If the diffusion behavior of potassium is similar to that of sodium, one has further evidence for disregarding the two-group concept of bcc metals.

## EXPERIMENTAL METHOD

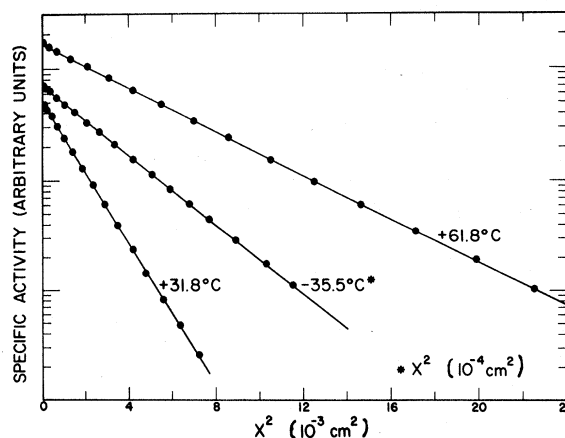The measurements were made in the same man-



FIG. 1.   Concentration profiles for diffusion of $^{42}K$ into potassium.